Journal of Materials Chemistry

Cite this: J. Mater. Chem., 2012, 22, 4312

www.rsc.org/materials

PAPER

Self-assembled monolayer and multilayer films based on L-lysine functionalized perylene bisimide†

Yan Sun, Zhibo Li* and Zhaohui Wang*

Received 12th September 2011, Accepted 26th October 2011
DOI: 10.1039/c1jm14521e

L-Lysine functionalized tetrachloroperylene bisimide (Lys-4ClPBI-Lys) was synthesized, and its aqueous self-assembly behaviours were investigated at different pH values. The zwitterionic-type Lys-4ClPBI-Lys amphiphile spontaneously self-assembled into a uniform monolayer film in water at pH ranging from 9 to 1, whereas it did not formed any ordered aggregates in solution with pH above 10. Formation of the monolayer film was believed due to synergistic interaction of directional π–π interactions and intermolecular hydrogen bonding. In contrast, the addition of copper(II) ions induced the formation of multilayer films due to inter-film ligation between Cu^{2+} and the α-amino acid moiety. The corresponding self-assembly behaviours and assemblies' structures were characterized using UV-vis absorption and fluorescence emission spectroscopy, cryogenic transmission electron microscopy, atomic force microscopy, and X-ray diffraction.

Introduction

Construction of highly ordered functional materials *via* self-assembly is of particular importance to optimize performance of semiconductor molecules.[1–3] Controllable self-assembly of organic conjugated macrocycle π-molecules recently emerged as a versatile platform to tune the properties of thin film materials and devices.[4] Compared to well-developed p-type semiconductors, preparing high-performance n-type materials remains a challenge. In particular, perylene bisimide (PBI) and its derivatives have received extensive research interests because of their outstanding optoelectronic properties as a unique class of n-type semiconductor.[5–7] Herein, we demonstrated a simple strategy to prepare two-dimensional monolayers and multilayers from a bolaamphiphile based on L-lysine functionalized tetrachloroperylene bisimide (Lys-4ClPBI-Lys).

Although a variety of supramolecular structures such as nanowires, nanobelts, nanorods, and vesicles, have been constructed from PBI derivatives with hydrophilic or hydrophobic segments attached at the PBI's imide position,[8–13] reports of forming 2-dimensional monolayer films are still rare. Moreover, amphiphilic surfactants derived from PBI were found to have great advantages with regard to stabilizing and solubilizing carbon nanotubes and graphene.[14,15] On the other hand, amino acids or oligopeptides as a structure-tuning moiety have recently received extensive research interests, because the amino acid can afford an array of hierarchical supramolecular structures with different degrees of ordering arising from their site-specific hydrogen bonding and secondary structures in addition to their inherent pH responsive properties. There have been several studies using oligopeptides to tune nanostructures of semiconductors. For example, Parquette and co-workers reported the self-assembly of oligopeptide functionalized naphthalene diimide,[16–18] and Chen *et al.*, studied the nanostructure control and electronic properties of oligopeptide conjugated anthracene.[19] Using amino acid as functional groups, Hirsch and co-workers synthesized chiral, water-soluble PBI derivatives.[20] Most recently, we studied the structure control of nanostructures using NαCBZ-Lysine functionalized 4ClPBI in an acetone/H_2O mixture.[21]

In this work, we selectively conjugate the ε-amine group of L-lysine to the imide position of 4ClPBI to obtain a symmetric bolaamphiphile with 4ClPBI as the hydrophobic core and lysine as hydrophilic heads. For bolaamphiphiles, the introduction of an amino acid plus amide bonds gave a rich structure variation compared to single head surfactants.[22–24] We find that Lys-4ClPBI-Lys self-assembled into 2-D monolayer film at pH ranging from 9 to 1 as revealed by cryoTEM and AFM. Addition of Cu^{2+} ions can bring monolayer films together to form multilayer films.

Experimental section

Materials

1,6,7,12-Tetrachloroperylene-3,4,9,10-tetracarboxylic acid dianhydride was purchased from commercial sources at analytical

Beijing National Laboratory for Molecular Sciences (BNLMS), Institute of Chemistry, Chinese Academy of Sciences, Beijing, 100190, China. E-mail: zbli@iccas.ac.cn; wangzhaohui@iccas.ac.cn; Fax: +8610-6256-5612; Tel: +8610-6256-5612

† Electronic supplementary information (ESI) available: zeta potential, additional UV-vis, SEM and TEM characterizations. See DOI: 10.1039/c1jm14521e

grade. NαBoc-L-lysine-OH was purchased from GL Biochem (Shanghai) Ltd. Other chemicals were purchased from Sinopharm Chemical Reagent Co, Ltd. and used without further purification, unless otherwise noted.

Synthesis

1,6,7,12-Tetrachloroperylene-3,4,9,10-tetracarboxylic acid dianhydride and NαBoc-L-lysine-OH were mixed with acetic acid, and the mixture was stirred at 75 °C for 24 h. After cooling to room temperature, orange Boc-Lys-4ClPBI-Lys-Boc precipitated when the mixture pH was adjusted to 1 using HCl. The orange precipitate then was filtered, washed successively with water, and dried in a vacuum oven. MALDI-TOF: $C_{46}H_{44}Cl_4N_4O_{12}$, calcd 984, obsd 984. IR (KBr disk) *v*: 3446, 2360, 2341, 1654, 1415, 1162, 669 cm^{-1}. For deprotection of the Boc groups, the orange product was dissolved in dichloromethane under stirring before adding trifluoroacetic acid (TFA). The mixture was stirred at RT for two days. The solution was then concentrated using a rotary evaporator, followed by neutralization using $NaHCO_3$ to give a red precipitate, which was isolated by filtration and washed with DI-water to give the final product Lys-4ClPBI-Lys. ^1H NMR (400 MHz, D_2O, TMS): δ 8.2 (br, 4H), 3.3–3.1 (m, 6H), 1.9–1.3(m, 12H). MALDI-TOF: $C_{36}H_{28}Cl_4N_4O_8$, calcd 784, obsd 784. IR (KBr disk) *v*: 3452, 2360, 1641, 1414, 546 cm^{-1}.

Characterizations

^1H NMR spectra were recorded on a Bruker Advance DMX 400 MHz. MALDI-TOF-MS measurements were carried out on Bruker BIFLEX III equipped with a 337 nm nitrogen laser. UV-vis absorption spectra (UV-vis) were recorded on a TV-1901 spectrophotometer. Fluorescence spectra were recorded on a Hitachi F-4500 fluorescence spectrometer and corrected against photomultiplier and lamp intensity. The slit width of both monochromators was 5.0 nm. Atomic Force Microscopy (AFM) was performed in tapping mode (Nanoscope IIIa, Digital Instruments, Inc.) using silicon cantilever probes. The scanning rate was usually 1 Hz. X-Ray diffraction (XRD) data were obtained with a graphite monochromatic device and Cu-Kα radiation ($\lambda = 0.15406$ nm) on the Rigaku D/max 2500, operated in the 3∼60° (2θ) range and with a step-scan of $2\theta = 0.04°$. The tube voltage was 40 kV, and the tube current was 200 mA. CryoTEM samples were prepared in a controlled environment vitrification system (CEVS) at 28 °C.[25] The vitrified samples were then stored in liquid nitrogen until they were transferred to a cryogenic sample holder (Gatan 626) and examined using a JEM2200FS TEM (200 kV) at about −174 °C. Regular TEM and AFM samples were prepared by casting dilute sample solution on carbon film and freshly peeled mica, respectively.

Sample preparation

Lys-4ClPBI-Lys was initially dissolved in 1 M NaOH solution to form a 1 mM stock solution. The stock solution was then diluted to 50 μM and predetermined pH values using DI water and NaOH or HCl solution. The obtained solutions were aged at room temperature for at least 3 days before being subjected to any measurements. For copper coordinated multilayers, copper dichloride aqueous solution (1 mM) was mixed with 100 μL Lys-4ClPBI-Lys solution (1 mM, pH = 11) to produce mixtures with different NH_2/Cu^{2+} ratios. After that, prescribed DI-water was added to adjust the solution concentration to 50 μM.

Results and discussion

Lys-4ClPBI-Lys was prepared *via* direct coupling between 1,6,7,12-tetrachloroperylene anhydride and NαBoc-L-lysine-OH in NMP at 75 °C followed by selective deprotection of the Boc group.[21] Its chemical structure is shown in Scheme 1. Its molecular structure was confirmed using NMR, FTIR, and MALDI-TOF. Apparently, Lys-4ClPBI-Lys mimics a bolaamphiphile structure with the hydrophobic rigid perylene backbone as skeleton and pH-responsive lysine residue as hydrophilic heads. Compared to a classical bolaamphiphile, Lys-4ClPBI-Lys contains a macro-aromatic ring, which provides strong π–π interactions in addition to hydrophobic effects. Hydrophilic lysine residues are zwitterions, which offer pH-dependent solubility. Lys-4ClPBI-Lys was found to be insoluble in most common organic solvents, but its apparent solubility in water was strongly influenced by the solution pH due to the zwitterionic nature of the lysine residue. Considering such a structural feature, we thus studied the self-assembly of Lys-4ClPBI-Lys in different pH solutions.

We firstly investigated the apparent charge of Lys-4ClPBI-Lys or its assemblies at different pH values using electrophoresis. The zeta potentials correlate to the pK_a values of the lysine ends, and reflect their ionization status at different pH (Fig. S1†).[26] Between pH = 14 and pH = 5, the zeta potential remains a relatively constant value of about −30 mV, which indicates that Lys-4ClPBI-Lys has negative charges when the pH is between 14 and 5. At pH = 3 or 4, the measured zeta potential is close to zero, indicating the isoelectric point for Lys-4ClPBI-Lys. On the other hand, we also found that the precipitate started to appear when the solution pH was tuned to 4. If we took the pK_a of –COOH and NH_3^+ being 2 and 8, we can estimate the ionization status of the –COOH groups and NH_2 groups as shown in Fig. S2.† At pH > 10, most –COOH groups disassociate into $–COO^-$ groups (Fig. S2b†). In this case, deprotonated NH_2 and $–COO^-$ groups coexist within the pH range of 10–4, however, with different ionization degrees. For the example of pH = 7, more than 99% NH_2 groups do not ionize, and only about 10% –COOH groups become $–COO^-$. In contrast, more than 99% NH_2 groups become NH_3^+ at pH = 1. Therefore, this ionization

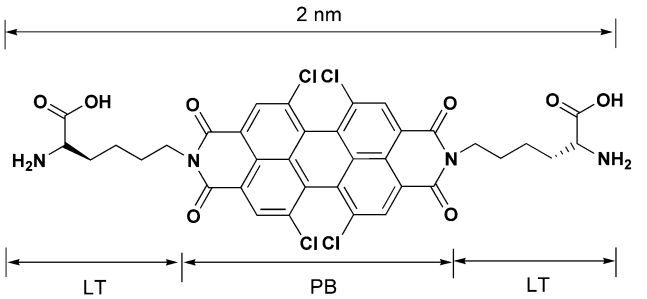

Scheme 1 Chemical structure of Lys-4ClPBI-Lys.

status will certainly affect the self-assembly behaviours of Lys-4ClPBI-Lys.

We initially noticed that the solution colour changed from green to orange and to pink at pH values of 14, 12, and 9, respectively. The aggregation status of Lys-4ClPBI-Lys in different pH solutions was firstly addressed using UV-vis and fluorescence spectroscopy (Fig. 1). Regardless of the solution pH, Lys-4ClPBI-Lys displays two characteristic absorption regions around the range of 260–290 nm (band II) and 350–600 nm (band I), which correspond to π–π* transitions polarized along the short and long axes of the PBI chromophore, respectively.[27] At pH = 14, Lys-4ClPBI-Lys only has a relatively narrow absorption between 350 and 480 nm, indicating the molecularly free status for Lys-4ClPBI-Lys.[5] When the solution pH was decreased from 14 to 12, two distinct absorption peaks showed up around 500 and 545 nm, accompanying an intensity decrease for absorptions at 446, 425 and 382 nm. Such variation generally was assumed to be the occurrence of molecular association. Further decrease of solution pH caused additional absorption intensity increase at 500 and 545 nm (Fig. 1a). The series of UV-vis absorption spectra *versus* pH variation reveal an isosbestic point at 464 nm indicating formation of ordered aggregates (Fig. S3†).[8,28] The UV-vis spectra of Lys-4ClPBI-Lys showed negligible changes between pH = 9 and pH = 1 except that Lys-4ClPBI-Lys slowly precipitated out at pH = 3 and 4. The reason we believe is that its isoelectric point is around 4, which can also be inferred from zeta potential measurements. Similar pH-induced self-assemblies of Lys-4ClPBI-Lys in water were further supported from fluorescence characterization. Fig. 1b presents the fluorescence spectra of Lys-4ClPBI-Lys at different pH solutions with a concentration of 50 μM. At pH 14, Lys-4ClPBI-Lys shows strong fluorescence at 490 nm. When the pH is decreased to 12, emission at 490 nm remains while a new peak at 569 nm shows up. This result implies a transition from free molecules to aggregated status for Lys-4ClPBI-Lys. At pH = 9, the emission intensity at 490 nm diminishes substantially accompanied with an intensity increase at 569 nm. Thus, these spectroscopy results indicate that Lys-4ClPBI-Lys starts to form ordered supramolecular assemblies when the pH is <10.

According to the above results, we then focused our studies on three representative pH values, *i.e.* pH = 14, 9, and 1, respectively, to explore their morphologies. The assemblies' nanostructures at different pH solutions were characterized using TEM and AFM. Note that cryoTEM is an excellent technique to determine the supramolecular nanostructures with great preservation of pristine structure in solution.[29,30] At pH = 14, no aggregates are observed by TEM as expected and agree well with UV-vis and fluorescence results. At pH = 9, Lys-4ClPBI-Lys forms thin film-like assemblies floating in water as demonstrated from cryoTEM measurements shown in Fig. 2a. These films range from a few hundred nanometres to a few micrometres. When we dry the sample solution on carbon film, and still

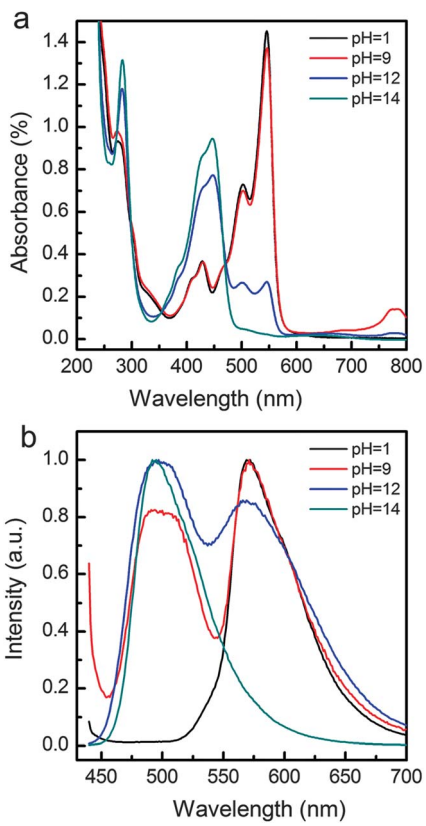

Fig. 1 UV-vis (a) and fluorescence (b) spectra of Lys-4ClPBI-Lys aqueous solution (c = 50 μM).

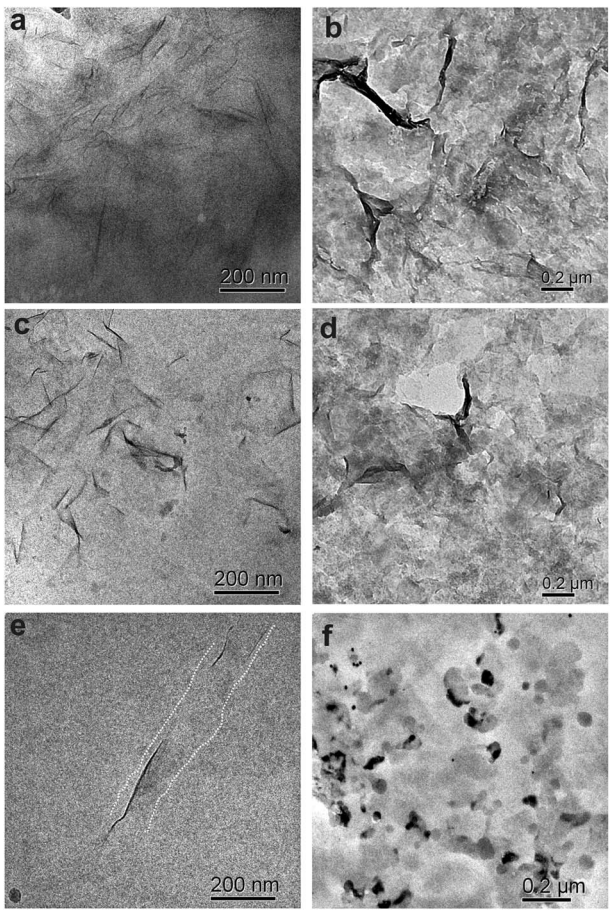

Fig. 2 Cryo-TEM images (a,c,e) and regular TEM images (b,d,f) of assemblies formed from Lys-4ClPBI-Lys at different pH solutions: (a,b) pH = 9, (c,d) pH = 6, and (e,f) pH = 1, respectively.

observe a large amount of flexible films stacked together as shown in Fig. 2b, which further confirms the film morphology. Since the determination of film thickness might reveal inherent correlation between the assembly structure and the molecular dimension, we applied AFM to study the film thickness under different conditions. The AFM samples were prepared by direct-casting an aliquot sample solution onto freshly peeled mica and air-drying. Fig. 3a shows the corresponding AFM height images for the sample in pH = 9 solution. Quantitative analysis from the indicated line-scan profile over an individual film in Fig. 3a gives a film thickness of about 1.8 nm. Moreover, Fig. 3a also shows some stacked films, on which line-scan profiles give a thickness of about 3.6 nm and 5.2 nm shown in Fig. 3b. These results suggest that the uniform film thickness is about 1.8 nm. Using molecules simulation, the extended molecular dimension along the long axis of Lys-4ClPBI-Lys is about 2 nm. Considering possible molecule collapse during sample preparation, we presume that the Lys-4ClPBI-Lys bolaamphiphile forms monolayers in solution at pH = 9.

The cryoTEM image shown in Fig. 2c reveals that Lys-4ClPBI-Lys formed dense films at pH = 6. Drying the solution sample on a carbon film still maintained the film structures, confirmed in the TEM shown in Fig. 2d. Meanwhile, it is found that the film dimensions decreased substantially at low pH such as pH = 1, from cryoTEM (Fig. 2e) and regular TEM (Fig. 2f). We also applied SEM to characterize the assembly morphology under dried status. Unfortunately, SEM measurements only show the collapsed layer structures without showing details (Fig. S4†). Moreover, the film morphology did not change with sample concentration as inferred from cryoTEM examination. Lys-4ClPBI-Lys still formed large film structures between 10 μM and 1 mM (Fig. S5†).

We have demonstrated that Lys-4ClPBI-Lys can self-assemble into monolayer films within an appropriate pH range. A question arises whether we can fabricate multilayer films from such well-defined monolayer films. It was known that α-amino acid can act as a ligand to form a five-membered ring complex with Cu^{2+} under basic conditions.[31,32] We thus added different amounts of Cu^{2+} into the sample solution at pH = 11, and investigated whether the addition of Cu^{2+} can result in the formation of multilayer films or not (Fig. 4 and Fig. S6†). TEM images of the dried sample show that Lys-4ClPBI-Lys with Cu^{2+} leads to the formation of large film structures (Fig. S6†). AFM characterizations reveal that the film thickness varies for samples with different NH_2/Cu^{2+} ratios (Fig. 4). When NH_2/Cu^{2+} = 1, the resulting films are about 10 nm thick (Fig. 4b), in which the representative film thicknesses are about 8, 6, and 12 nm, respectively, corresponding to 4–6 layers of Lys-4ClPBI-Lys monolayers. In the above case, the Cu^{2+} is the limiting species as one Cu^{2+} ion needs to complex two NH_2 groups. If we used two-fold of NH_2 groups over the Cu^{2+} ions (NH_2/Cu^{2+} = 2), thicker films are expected compared to the previous case (Fig. 4c). Quantitative examinations reveal that those multilayer films are about 22 and 26 nm thick (Fig. 4d). If we used excess Cu^{2+}, the film thickness increased to about 140, 156 and 152 nm (Fig. 4e–f). These results demonstrate that we can use this strategy to fabricate multilayer semiconductor films.

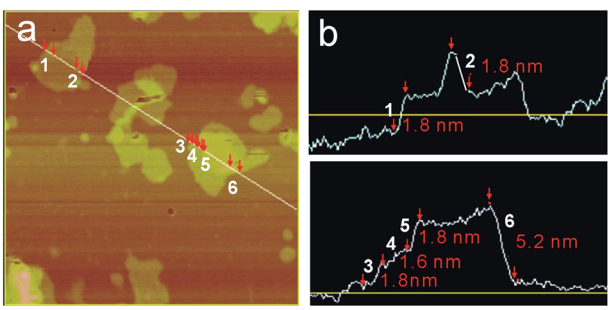

Fig. 3 AFM height image (a) and thickness profile (b) of supramolecular films formed by Lys-4ClPBI-Lys (50 μM, pH = 9).

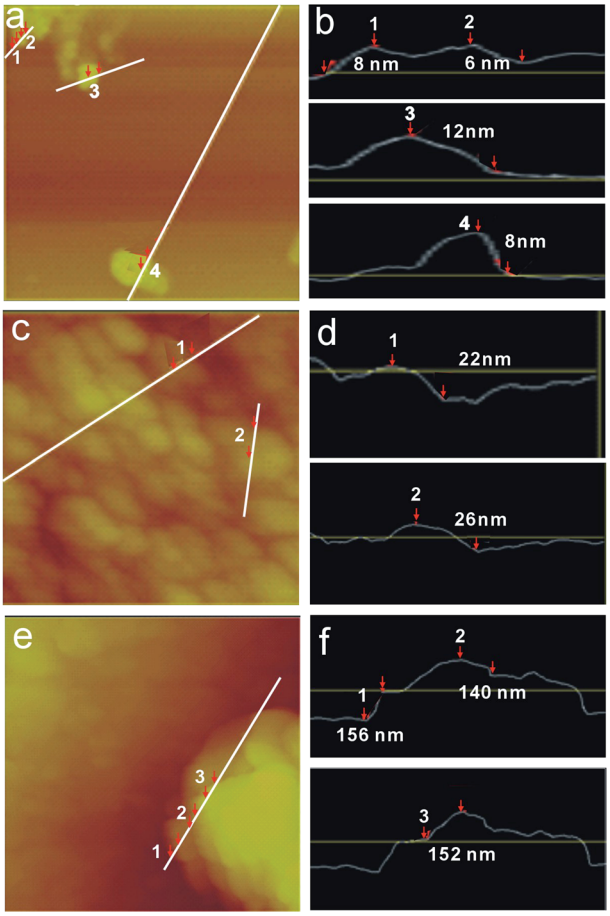

Fig. 4 AFM image of multilayer formed by the addition of Cu^{2+} at different NH_2/Cu^{2+} ratio: (a,b) 1, (c,d) 2, and (e,f) 4.

Above all, the target Lys-4ClPBI-Lys mimics a zwitterionic type bolaamphiphile featured with an α-amino acid head and rigid perylene bisimide as the backbone (Scheme 1). It was known that macro-aromatic molecules such as perylene bisimide intended to form zero- or one-dimensional supramolecular assemblies such as nanospheres, nanobelts and nano-ribbons.[9,11,12,28] Whereas, large two-dimensional films are still rare for such systems. Hence, it would be critical to understand the underlying mechanism to pave avenues for even higher ordered structures *via* controlled self-assembly. We thus propose a possible mechanism illustrated in Scheme 2. The self-assembly of Lys-4ClPBI-Lys in aqueous solution is supposed to be affected by many factors including electrostatic interactions, hydrogen

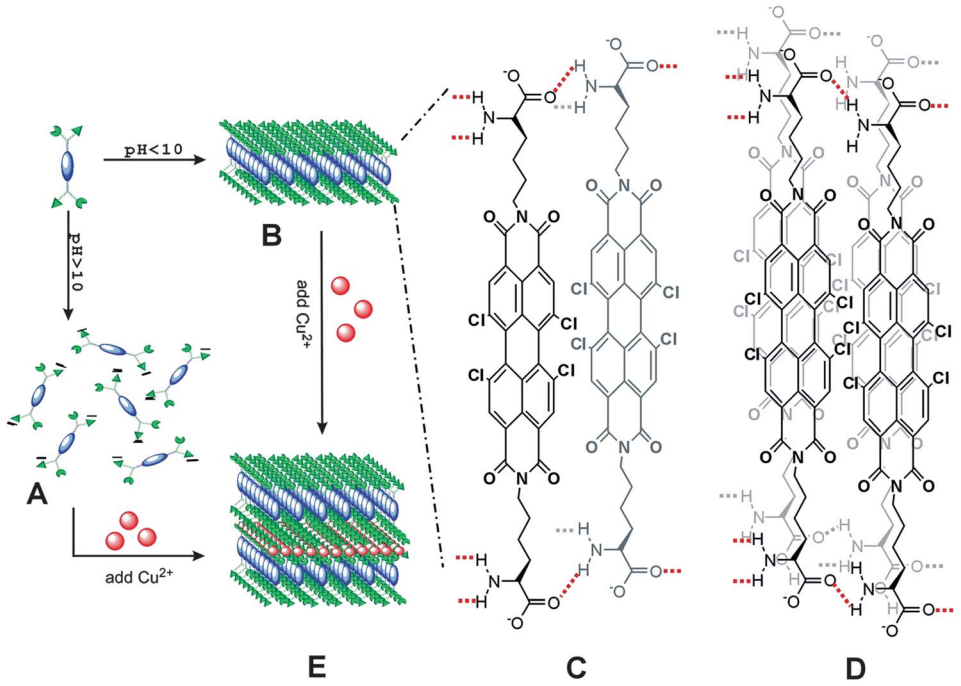

Scheme 2 Schematic illustration of self-assembly mechanism for Lys-4ClPBI-Lys monolayer films and Cu^{2+} mediated formation of multilayer films.

bonding, hydrophobic and π–π interactions. The former two factors are determined by the solution pH values and ionic strength. If we used $pK_1 = 2$ and $pK_2 = 8$ as the pK_a of the carboxylic acid group and the α-amine of lysine, respectively, we can estimate the ionizing status for each functional group at a particular pH (Fig. S2†). At high pH, *i.e.*, pH > 10, more than 99% –COOH groups exist in the form of $–COO^-$. The electrostatic repulsion thus dominates the interactions between individual Lys-4ClPBI-Lys molecules, and causes disassociation of Lys-4ClPBI-Lys aggregates (Scheme 2A). Therefore, no supramolecular assemblies are observed in such basic solutions. Decrease of the solution pH, *e.g.*, 4 < pH < 10, both amine and carboxylic acid are partially dissociated. Concomitantly, the intermolecular electrostatic repulsion is weakening, while the intermolecular hydrogen bonding between amine and carboxylic acid groups is promoted and leads to self-assembly of Lys-4ClPBI-Lys. In addition, the 4ClPBI backbone prefers cofacial π–π stacking, so random irregular structures are disfavoured. Also, the partial electrostatic repulsions suppress the formation of multilayers. Consequently, the Lys-4ClPBI-Lys interacts to form a 2-D monolayer film considering a balance of π–π interactions, hydrogen bonding and ionic interactions as illustrated in Scheme 2B. In particular, Scheme 2C illustrates the hydrogen bonding along the direction of cofacial π–π interactions, while Scheme 2D illustrates the hydrogen bonding parallel to the perylene aromatic ring. Although the change of solution ionic strength would screen the electrostatic repulsions, for which we did not perform systematic studies in this study, we believed that such an effect would not change the overall self-assembly behaviours. Further decrease in the solution pH does not change the overall assembly morphology until reaching the isoelectric point, where electrostatic attraction dominates the interactions to induce disordered aggregation and phase separation. At strong acidic pH, amine groups become fully charged, and –COOH groups become protonated. The regained electrostatic repulsion prevents the formation of ionic complexes. Meanwhile, $–NH_3^+$ and –COOH can form hydrogen bonding, however, to a lesser extent compared to neutral pH. We thus only observe small pieces of monolayer films as revealed by the cryoTEM and TEM images shown in Fig. 2e and 2f. As we propose in Scheme 2, a monolayer film is generally formed due to the net surface charge on either film. Another idea emerges as to whether we can bring together layers using multivalent ions. We then tried to use copper(II) as a bridge to link multiple layers together. Cu^{2+} is chosen owing to its strong interaction with amino acids and thus enables the formation of complexes under basic conditions.[33] Depending on the molar ratio between NH_2 groups and Cu^{2+} groups, the Lys-4ClPBI-Lys monolayers can reassemble into multilayers as discussed in the previous section, which further supports our self-assembly mechanism shown in Scheme 2.

The above-proposed mechanism is also supported from our experimental results. At pH = 14, UV-vis and fluorescence spectra indicate a disassociated status for Lys-4ClPBI-Lys, while supramolecular aggregates appear, as inferred from new absorption and emission spectra when the pH is decreased to 10. Furthermore, both cryoTEM and regular TEM characterization demonstrated the above conclusion that no aggregates were found at pH 14. At the pH ranging from 9 to 1, a large amount of films was observed. The uniform film thickness as observed by AFM was about 1.8 nm, which is close to the extended molecular length of Lys-4ClPBI-Lys. The intermolecular interactions at different statuses were also characterized using FTIR (Fig. 5a), from which we can infer hydrogen bonding information from the C═O and N–H stretching vibration bands.[34] For the powder sample prior to self-assembly, FTIR finds the amide I and amide

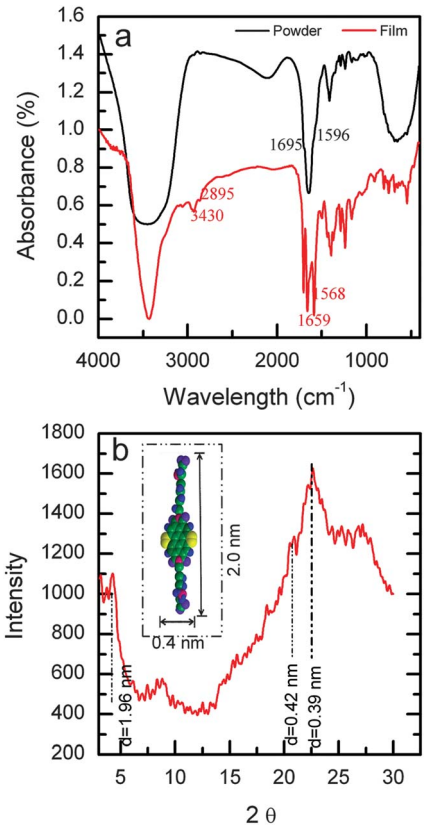

Fig. 5 (a) FT-IR spectra of Lys-4ClPBI-Lys powder and film, (b) XRD profile of supramolecular film.

II bands are at 1695 and 1596 cm^{-1}. In contrast, that the amide I and II bands for Lys-4ClPBI-Lys film are at 1659 (νC=O) and 1568 cm^{-1} (δN–H), respectively. The decrease of wave numbers suggests the enhancement of the hydrogen-bonding strength and also demonstrates that strong and orderly hydrogen bonds are formed in the assemblies.[35] Furthermore, the strong bands at 2931 and 2895 cm^{-1} also imply ordered hydrocarbon chains within the assemblies as these vibrational bands are very sensitive to the packing degree of the alkyl chain.[34] These results show that intermolecular hydrogen bonds exist within the Lys-4ClPBI-Lys molecules. Further evidence is provided by XRD, which shows a *d*-spacing of 1.96 nm and 0.42 nm (Fig. 5b). The data are close to the extended length and width of Lys-4ClPBI-Lys, which indicated long-range ordering.[36] Furthermore, the *d*-spacing corresponding to the cofacial intermolecular stacking is observed at 0.39 nm in agreement with the π–π stacking distance between perylene bisimides.

Conclusion

In summary, the synthesis and self-assembly of L-lysine functionalized tetrachloroperylene bisimide was reported. The target Lys-4ClPBI-Lys mimicked a zwitterionic-type bolaamphiphile featured with an α-amino acid head and rigid perylene bisimide as backbone. Depending on the solution pH, Lys-4ClPBI-Lys dissolved in strong alkaline solution, *i.e.*, pH > 10, whereas it self-assembled into monolayer films at pH values between 9 and 1. The formation of monolayer films was believed due to the synergistic interaction of directional π–π interactions and intermolecular hydrogen bonding. Such pH-controlled self-assembly opened a new strategy to prepare large, two-dimensional semiconductor films. Furthermore, multilayer films could be formed by the addition of Cu^{2+} ions, which led to the formation of complexes between Cu^{2+} and the amino acid. Our strategy also provided a possible way to make hierarchical multilayer films *via* a layer-by-layer strategy using semiconductor building blocks and transition metal ions. The electronic properties of these multilayer films are currently under investigation.

Acknowledgements

The authors appreciate financial support from the National Natural Science Foundation of China (91027043) and National Basic Research Program of Ministry of Science and Technology of China (2012CB933200, 2011CB932301).

Notes and references

1 L. Zang, Y. K. Che and J. S. Moore, *Acc. Chem. Res.*, 2008, **41**, 1596–1608.
2 Y. Guo, C. Du, G. Yu, C.-a. Di, S. Jiang, H. Xi, J. Zheng, S. Yan, C. Yu, W. Hu and Y. Liu, *Adv. Funct. Mater.*, 2010, **20**, 1019–1024.
3 R. Li, W. Hu, Y. Liu and D. Zhu, *Acc. Chem. Res.*, 2010, **43**, 529–540.
4 K. Sakakibara, J. P. Hill and K. Ariga, *Small*, 2011, **7**, 1288–1308.
5 F. Würthner, *Chem. Commun.*, 2004, 1564–1579.
6 Z. Chen, M. G. Debije, T. Debaerdemaeker, P. Osswald and F. Würthner, *ChemPhysChem*, 2004, **5**, 137–140.
7 F. Würthner, *Pure Appl. Chem.*, 2006, **78**, 2341–2349.
8 J. H. Oh, H. W. Lee, S. Mannsfeld, R. M. Stoltenberg, E. Jung, Y. W. Jin, J. M. Kim, J. B. Yoo and Z. N. Bao, *Proc. Natl. Acad. Sci. USA*, 2009, **106**, 6065–6070.
9 X. Zhang, S. Rehm, M. M. Safont-Sempere and F. Würthner, *Nat. Chem.*, 2009, **1**, 623–629.
10 A. L. Briseno, S. C. B. Mannsfeld, C. Reese, J. M. Hancock, Y. Xiong, S. A. Jenekhe, Z. Bao and Y. Xia, *Nano Lett.*, 2007, **7**, 2847–2853.
11 Y. K. Che, A. Datar, K. Balakrishnan and L. Zang, *J. Am. Chem. Soc.*, 2007, **129**, 7234–7235.
12 Y. K. Che, X. M. Yang, G. L. Liu, C. Yu, H. W. Ji, J. M. Zuo, J. C. Zhao and L. Zang, *J. Am. Chem. Soc.*, 2010, **132**, 5743–5750.
13 K. Balakrishnan, A. Datar, R. Oitker, H. Chen, J. M. Zuo and L. Zang, *J. Am. Chem. Soc.*, 2005, **127**, 10496–10497.
14 C. Backes, F. Hauke and A. Hirsch, *Adv. Mater.*, 2011, **23**, 2588–2601.
15 C. Backes, C. D. Schmidt, K. Rosenlehner, F. Hauke, J. N. Coleman and A. Hirsch, *Adv. Mater.*, 2010, **22**, 788–802.
16 H. Shao, J. Seifert, N. C. Romano, M. Gao, J. J. Helmus, C. P. Jaroniec, D. A. Modarelli and J. R. Parquette, *Angew. Chem., Int. Ed.*, 2010, **49**, 7688–7691.
17 H. Shao and J. R. Parquette, *Angew. Chem., Int. Ed.*, 2009, **48**, 2525–2528.
18 H. Shao, T. Nguyen, N. C. Romano, D. A. Modarelli and J. R. Parquette, *J. Am. Chem. Soc.*, 2009, **131**, 16374–16376.
19 Y. Sun, L. Jiang, K. C. Schuermann, W. Adriaens, L. Zhang, F. Y. C. Boey, L. De Cola, L. Brunsveld and X. Chen, *Chem.–Eur. J.*, 2011, **17**, 4746–4749.
20 C. D. Schmidt, C. Bottcher and A. Hirsch, *Eur. J. Org. Chem.*, 2009, 5337–5349.
21 Y. Sun, C. He, K. Sun, Y. Li, H. Dong, Z. Wang and Z. Li, 2011, **27**, 11364–11371.
22 T. Wang, J. Jiang, Y. Liu, Z. Li and M. Liu, *Langmuir*, 2010, **26**, 18694–18700.
23 C. D. Meglio, S. B. Rananavare, S. Svenson and D. H. Thompson, *Langmuir*, 2000, **16**, 128–133.
24 J.-H. Fuhrhop and T. Wang, *Chem. Rev.*, 2004, **104**, 2901–2938.
25 J. R. Bellare, H. T. Davis, L. E. Scriven and Y. Talmon, *J. Electron Microsc. Tech.*, 1988, **10**, 87–111.

26 R. Folkersma, A. J. G. van Diemen and H. N. Stein, *Langmuir*, 1998, **14**, 5973–5976.
27 M. Sadrai, L. Hadel, R. R. Sauers, S. Husain, K. Kroghjespersen, J. D. Westbrook and G. R. Bird, *J. Phys. Chem.*, 1992, **96**, 7988–7996.
28 K. Balakrishnan, A. Datar, T. Naddo, J. L. Huang, R. Oitker, M. Yen, J. C. Zhao and L. Zang, *J. Am. Chem. Soc.*, 2006, **128**, 7390–7398.
29 Z. Li, E. Kesselman, Y. Talmon, M. A. Hillmyer and T. P. Lodge, *Science*, 2004, **306**, 98–101.
30 H. Cui, T. K. Hodgdon, E. W. Kaler, L. Abezgauz, D. Danino, M. Lubovsky, Y. Talmon and D. J. Pochan, *Soft Matter*, 2007, **3**, 945–955.
31 N. C. Li and E. Doody, *J. Am. Chem. Soc.*, 1954, **76**, 221–225.
32 N. C. Li and E. Doody, *J. Am. Chem. Soc.*, 1952, **74**, 4184–4188.
33 R. Buller, H. Cohen, T. R. Jensen, K. Kjaer, M. Lahav and L. Leiserowitz, *J. Phys. Chem. B*, 2001, **105**, 11447–11455.
34 M. Kogiso, S. Ohnishi, K. Yase, M. Masuda and T. Shimizu, *Langmuir*, 1998, **14**, 4978–4986.
35 M. R. Ghadiri, J. R. Granja, R. A. Milligan, D. E. McRee and N. Khazanovich, *Nature*, 1993, **366**, 324–327.
36 B. A. Jones, A. Facchetti, M. R. Wasielewski and T. J. Marks, *Adv. Funct. Mater.*, 2008, **18**, 1329–1339.

